RAPID COMMUNICATIONS IN MASS SPECTROMETRY
Rapid Commun. Mass Spectrom. 2006; **20**: 1648–1652
Published online in Wiley InterScience (www.interscience.wiley.com) DOI: 10.1002/rcm.2489

Comparison of the fragmentation pattern induced by collisions, laser excitation and electron capture. Influence of the initial excitation

R. Antoine[1], M. Broyer[1], J. Chamot-Rooke[2], C. Dedonder[3], C. Desfrançois[4], P. Dugourd[4], G. Grégoire[4], C. Jouvet[3], D. Onidas[5], P. Poulain[1], T. Tabarin[1] and G. van der Rest[2]

[1]Laboratoire de Spectrométrie Ionique et Moléculaire, UMR 5579 (Université Lyon I et CNRS), 43 Bd du 11 Novembre 1918, 69622 Villeurbanne cedex, France
[2]Laboratoire des Mécanismes Réactionnels, CNRS UMR 7651, Ecole Polytechnique, 91128 Palaiseau cedex, France
[3]Laboratoire de Photophysique Moléculaire du CNRS - Université Paris 11, Bât. 210, 91405 Orsay, France
[4]Laboratoire de Physique des Lasers du CNRS - Université Paris 13, Institut Galilée, 93430 Villetaneuse, France
[5]Laboratoire des Collisions Atomiques et Moléculaires CNRS - Université Paris 11, 91405 Orsay, France

Received 24 November 2005; Revised 13 March 2006; Accepted 15 March 2006

Collision-induced dissociation, laser-induced dissociation and electron-capture dissociation are compared on a singly and doubly protonated pentapeptide. The dissociation spectrum depends on the excitation mechanism and on the charge state of the peptide. The comparison of these results with the conformations obtained from Monte Carlo simulations suggests that the de-excitation mechanism following a laser or an electron-capture excitation is related to the initial geometry of the peptide. Copyright © 2006 John Wiley & Sons, Ltd.

The study of the fragmentation of polypeptides is of fundamental interest and may also have important applications in analytical sciences. A range of experiments in the area of proteomics rely on the identification of a peptide through the observation of its fragmentation pattern. A better understanding of the different mechanisms involved between the initial excitation event and the experimentally observed fragmentation in a tandem mass spectrometry (MS/MS) experiment on a peptide might allow the development of new strategies for peptide analysis in mass spectrometry.

Different methods are available to excite and fragment molecules. In low-energy collision-induced dissociation (CID) and infrared multiphoton dissociation (IRMPD), the peptide is heated in a multistep process. The model of the mobile proton can rationalize the observed fragments: the transfer of a proton weakens locally the peptide bond, which leads mainly to *a*-, *b*-, and *y*-type fragments. Since the fragmentation occurs after heating and vibrational energy redistribution, structural rearrangements are in competition with the fragmentation pathways. Therefore, the secondary or tertiary structures of the peptide cannot generally be revealed by means of low-energy CID experiments.

In contrast, electron-capture dissociation (ECD) and UV laser-induced dissociation (LID) are thought to induce non-ergodic cleavage,[1–3] i.e. bond breaking occurring faster than energy redistribution over all degrees of freedom. In ECD, a thermal electron neutralizes a proton. It is a one-step excitation leading to the formation of an hypervalent structure with an excess energy of about 5 eV in the peptide.[4] This leads to the formation of a hydrogen atom which is transferred to a nearby carbonyl group of the backbone and induces dissociation in *c*/*z*-type fragments.[5,6] Zubarev *et al.* showed that intramolecular weak bonding can be preserved upon ECD on bovine ubiquitin.[7] Furthermore, folding and unfolding of multiply charged peptides has also been characterized by ECD,[8,9] which highlights that non-ergodic fragmentation processes can reveal secondary and tertiary structures of the studied peptides.[10–12]

In LID, the photon induces an electronic excitation of the peptide. After excitation, direct dissociation in the excited state competes with internal conversion to the electronic ground state and with radiative de-excitation. At 266 nm (4.66 eV), electrons from the aromatic residues can be excited and a model that involves a charge transfer to a dissociative excited state has been proposed.[13,14] The excited state lifetimes of tryptophan and tryptophan-containing peptides measured by means of a femtosecond pump/probe scheme are short, in the range of hundreds of femtoseconds to tens of picoseconds, revealing a strong coupling of the locally excited $\pi\pi^*$ state with the predissociative state. Furthermore, specific fragmentation channels are detected, namely formation of radical cations following a H atom loss and C_α–C_β bond cleavage fragments.[2,15,16] At higher energy (157 nm, 7.9 eV), additional fragments similar to those observed in ECD are also observed.[17]

Correspondence to: P. Dugourd, Laboratoire de Spectrométrie Ionique et Moléculaire, UMR 5579 (Université Lyon I et CNRS), 43 Bd du 11 Novembre 1918, 69622 Villeurbanne cedex, France.
E-mail: dugourd@lasim.univ-lyon1.fr
Contract/grant sponsor: GDR CNRS; contract/grant number: 2758.

From these experimental findings, it is clear that the excitation mechanism has a strong influence on the produced fragments. While not specifically taken into account in models, the secondary structure of the peptide may also have an influence on the relaxation processes following an electronic excitation. In order to gain insight into structural and fragmentation properties of peptides, we have undertaken an exhaustive study of a pentapeptide, Ala-Gly-Trp-Leu-Lys, by means of several experimental methods, CID, ECD and LID. AGWLK was chosen because it contains a tryptophan residue needed for efficient UV excitation and a basic C-terminal amino acid, lysine, necessary to form doubly charged species. In parallel to the experiments, Monte Carlo simulations using AMBER force field functional have been performed to explore the ground state potential energy surface (PES) of the singly and doubly charged pentapeptides. Gas-phase conformations of the pentapeptide show differences upon the charge states. These differences in conformation are a possible explanation for the experimental findings.

EXPERIMENTAL

Ala-Gly-Trp-Leu-Lys was purchased from NeoMPS (Strasbourg, France) and used without further purification. Three different instruments were used. The first instrument is a Fourier transform ion cyclotron resonance instrument (FT-ICR, Bruker APEX III, Bremen, Germany) that was used for ECD and CID (SORI/CID mode with xenon) measurements. The second one is a quadrupole ion trap (QIT, LCQ Thermo Finnigan) which was modified to permit the injection of a tuneable nanosecond OPO laser.[18] It was used for LID and CID (with helium as buffer gas) experiments. The third instrument, also used for LID measurements, is an ion beam which crosses a 266 nm 100 femtoseconds or 100 nanoseconds laser beam.[19]

RESULTS AND DISCUSSION

Full-scan electrospray of Ala-Gly-Trp-Leu-Lys consists mainly of the singly $[M+H]^+$ and doubly charged $[M+2H]^{2+}$ molecular ions at m/z 574 and 288. Figure 1 shows CID and LID MS^2 spectra of protonated Ala-Gly-Trp-Leu-Lys (m/z 574). These spectra were obtained with the QIT experiment. The CID spectrum (Fig. 1(a)), which exhibits *b*-, *y*- and *a*-type fragments, is similar to the one with the SORI/CID mode of the FT-ICR experiment (data not shown). The LID spectrum obtained at $\lambda = 260$ nm (Fig. 1(b), nanosecond laser pulse) displays a prominent fragment originating from the neutral loss of one water molecule and b_3 and b_4 ions. The fragment at m/z 444 (loss of 130 Da) originates from the cleavage of the tryptophan side chain. This radical cation, which is not observed in CID, is a common fragment in LID experiments. Similar fragments were observed with femtosecond laser pulses in the cross-beam experiment while detected at a shorter time window (μs time scale). The LID spectrum observed following excitation at $\lambda = 220$ nm (Fig. 1(c)) exhibits two main fragmentation channels: m/z 573 (loss of 1 Da) and 444 (loss of 130 Da). The fragment ion m/z 573 corresponds to the loss of a hydrogen atom resulting in the formation of the radical $M^{+\cdot}$ ion. m/z 444 corresponds to the tryptophan side-chain cleavage already observed at $\lambda = 260$ nm. The fragments induced at 260 nm are still detected at 220 nm but to a lower extent than the two main fragments.

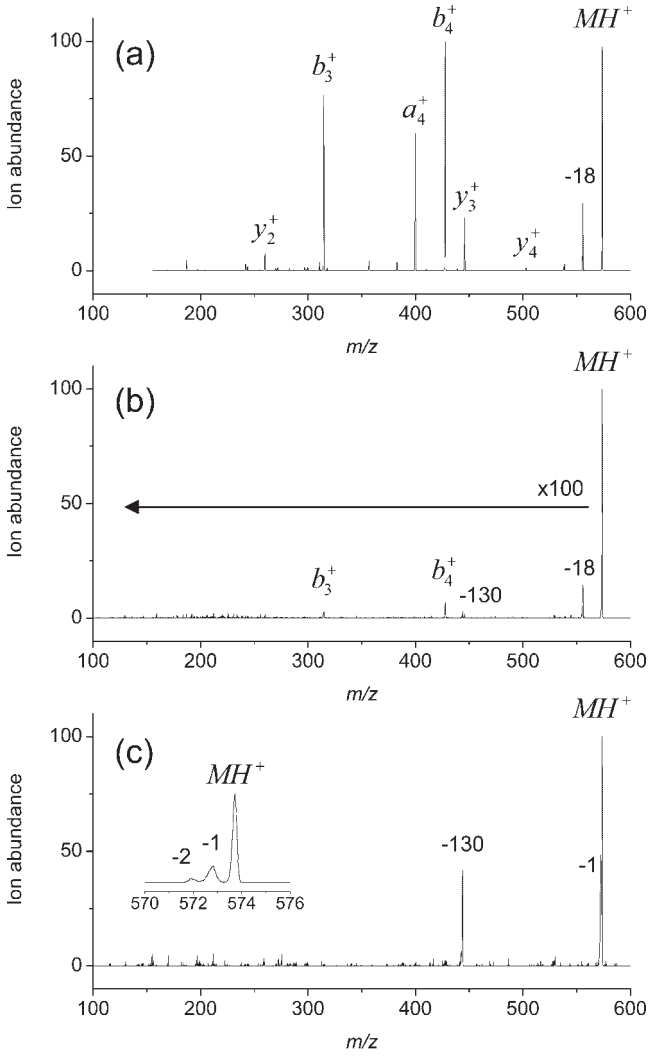

Figure 1. (a) CID, (b) LID at $\lambda = 260$ nm, and (c) LID at $\lambda = 220$ nm MS^2 spectra of [Ala-Gly-Trp-Leu-Lys+H]$^+$. The insert in (c) is a spectrum obtained in the zoom scan mode and showing hydrogen losses.

For the doubly protonated pentapeptide the CID spectrum displayed in Fig. 2 leads to the usual backbone cleavages (*a*, *b* and *y* ions). In contrast, for the LID spectrum (given in Fig. 2(b)), no or very little fragmentation is observed following excitation at $\lambda = 220$ nm. The same result (very low yield of fragmentation) was observed at $\lambda = 260$ nm, with both nanosecond and femtosecond laser pulses (the same laser conditions were used for both charge states). For these two wavelengths the fragmentation efficiency is estimated to be 50 times smaller for the doubly charged species than for the singly charged one. Finally, the ECD MS^2 spectrum (Fig. 2(c)) is dominated by *a*, *b* and *y* ions along with the singly protonated pentapeptide and a w_2 ion. No *c* or *z* ions were observed as would be expected in ECD. Moreover, with the exception of the w_2 ion, this fragmentation mass spectrum is

DOI: 10.1002/rcm

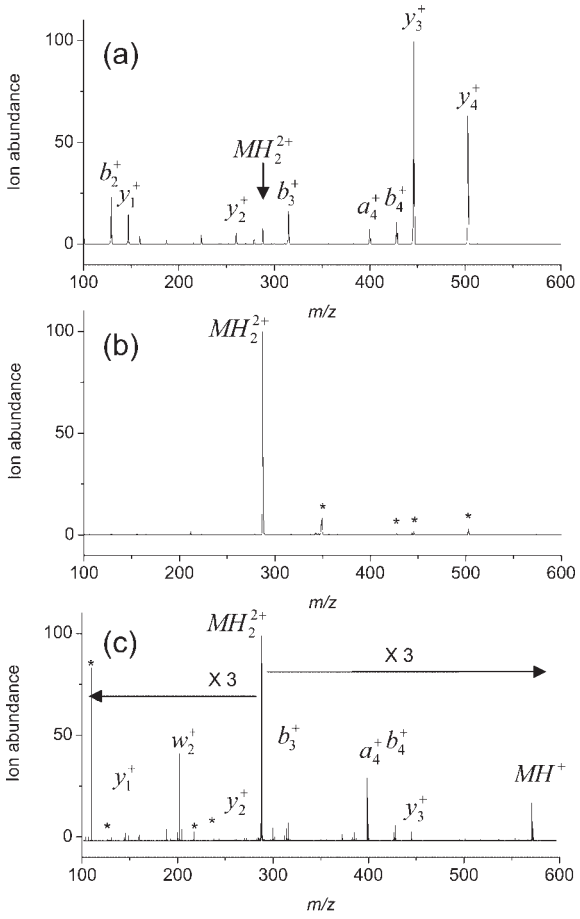

Figure 2. (a) CID, (b) LID at $\lambda = 220$ nm, and (c) ECD MS^2 spectra of [Ala-Gly-Trp-Leu-Lys $+2H]^{2+}$. In (b), the peaks labelled with asterisks were also observed without the laser and in (c) the peaks labelled with asterisks are noise peaks.

nearly the same, in both the ions present and their respective intensity ratios, as the CID spectrum of the singly charged peptide.

The results shown in Figs. 1 and 2 demonstrate, on a simple peptide, that the fragmentation patterns strongly depend on the method used to deposit energy in the peptide: collision (CID and SORI/CID), LID and ECD lead to different channels. They also depend on the electronic state excited by the photon as illustrated, e.g., in Figs. 1(b) and 1(c). The variety of channels that can be observed and the sensitivity to the excitation process emphasize the difficulty in building a general model for peptide fragmentation. In particular, Rice-Ramsperger-Kassel-Marcus (RRKM) simulations show that the energy of a single photon is not sufficient to induce significant fragmentation on the time scale of the experiment if a complete IVR had occurred. This means that the dynamics in the excited states should be taken into account or that complete IVR does not occur.

The most surprising results of these experiments are: the difference in the LID yields observed between the singly and doubly protonated peptide (the difference in the fragmentation yield is about one to two orders of magnitude) and the absence of *c* or *z* ions in the ECD spectrum. The difference in LID yields between the singly and doubly protonated pentapeptide could be explained by a difference in the absorption cross-section. The absorption is mainly due to a $\pi\pi$–$\pi\pi^*$ transition on the indole chromophore and the energy of this transition seems to be insensitive to the environment: gas-phase Trp, $[TrpH]^+$, tryptophan-containing peptide and Trp in solution[18,20–24] absorb in the same energy region. Moreover, the doubly protonated peptide does not fragment when excited at $\lambda = 260$ nm or at $\lambda = 220$ nm. If a weak $\pi\pi$–$\pi\pi^*$ absorption is responsible for the low fragmentation yield of the doubly charged peptide, the transition has to shift by more than 1 eV, which seems unlikely.

We propose an interpretation based on a general mechanism which emerges from previous work on the photodissociation of simple amino acids and a tryptophan-containing dipeptide.[13,14,19] In the model, the fragmentation mechanism is triggered by the coupling of the $\pi\pi^*$ excited state localized on the indole ring with a Rydberg-like dissociative $\pi\sigma^*$ state where the electron is localized on the protonated amino group: this can be viewed as an electron transfer from the indole ring to the C-NH_3^+ group. The localization of the electron on this group leads to the formation of a hypervalent C-NH_3 radical similar to the ammonium radical NH_4. This radical is unstable and undergoes fast dissociation along the NH coordinate.[25] The result can be either an H atom loss or internal conversion through a crossing between the $\pi\sigma^*$ state and the electronic ground state. In the absence of this process no fragmentation occurs. Since the electronic coupling between the $\pi\pi^*$ state and the $\pi\sigma^*$ state is strongly dependent on the distance between the indole ring and the protonated amino group, an efficient coupling occurs only if the NH_3^+ group is near the indole ring. In the framework of this model, even if the time scale for the appearance of the fragment ions may be long, the first step toward a specific fragmentation is short and depends on the initial geometry of the peptide.

Using this model, the huge variation in fragmentation efficiency between the singly and the doubly charged peptide is tentatively explained through differences in conformation. It is common sense that electrostatic repulsion between the two charges on the doubly protonated peptide may favor less compact structures as compared to the singly charged peptide. Monte Carlo calculations implemented with the replica exchange method (REM)[26,27] using Amber96 functional[28] (with $\varepsilon = 2$ for the electrostatic terms) were used to explore the PES of the singly and doubly protonated peptides. The singly charged peptide was protonated on the lysine side chain. For the doubly charged peptide, the second proton was added at the N-terminal group. These are the two most basic sites of the peptide and the most probable sites of protonation. We performed REM simulations of 6000000 Monte Carlo sweeps with nine replicas at temperatures 180, 206, 302, 380, 474, 588, 725, 893 and 1100 K. Replica-exchanges were attempted after periods of 100 Monte Carlo sweeps. Our simulations are initiated with a random conformation and the first 300000 Monte Carlo sweeps are used for thermalization and are not included in statistics. During each Monte Carlo sweep, we updated every dihedral angle on the peptide backbone and on the side chains (this represents a total of 25 dihedral angles). Bond lengths and

DOI: 10.1002/rcm

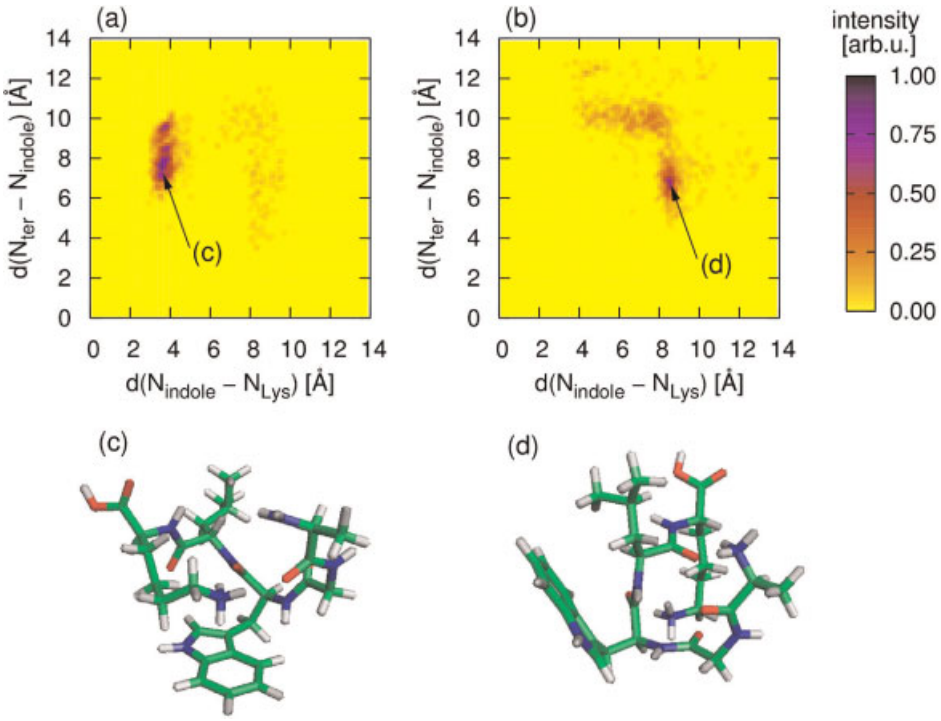

Figure 3. (a, b) Three-dimensional plots of the repartition of the structures obtained for the singly (a) and doubly (b) protonated peptide at 302 K (obtained from the REM simulations). Results are plotted as a function of (N_{indole}–N_{Lys}) and (N_{ter}–N_{indole}) distances. (c) Representative structure of the maximum observed in (a). (d) Representative structure of the maximum observed in (b).

angles were kept constant. During these simulations, we monitored the distances between the indolic nitrogen and the nitrogen atoms of the protonation sites, lysine group ($d(N_{indole}–N_{Lys})$) and N-terminal group ($d(N_{ter}–N_{indole})$). The results are plotted in Fig. 3. The different zones populated on these maps correspond to different families of structures. The coupling between the $\pi\pi^*$ state and the $\pi\sigma^*$ state can only occur for structures where one charge is close to the indole ring. For the singly charged peptide, the most probable structure is a folded structure where the protonated nitrogen is in interaction with the indole ring (Fig. 3(c)), so that an efficient charge transfer can occur. For the doubly protonated peptide, there is no clear maximum corresponding to structures with a charge in close interaction with the indole ring. The maximum in the map corresponds to structures where the two protons are partially solvated by carbonyl groups, without direct interaction between the charges and the indole ring: on average the indole-proton distance is longer and then the charge transfer cannot occur. While results of force field calculations should be considered with caution, these different secondary structures may account for the difference in the efficiency of the coupling between $\pi\pi^*$ and $\pi\sigma^*$ excited states and thus the difference in the fragmentation yield.

The structures observed for the doubly protonated peptide might also explain the results of ECD. The observation of *a*, *b*, *y* and *w* ions along with *c* and *z* ions has been described for 'hot-ECD' experiments,[29] where electrons with an energy on the order of 10 eV or more are used. In a recent work on the appearance of *b* ions in ECD spectra, Cooper[30] has shown that these fragmentations do not arise from secondary fragmentation of the *c* ions, and suggests that a mechanism for the appearance of these fragments could be energy deposition followed by H atom loss. Our results comfirm this hypothesis: in the case of the AGWLK peptide, no *c* or *z* ions were observed at all, and varying the electron energy from 1 to 16 eV did not alter noticeably the fragmentation ratios. One could hypothesize that the small size of the peptide might be a cause for this observed discrepancy: higher electron affinity brought by the presence of two close positive charges and redistribution of the recombination energy on fewer degrees of freedom could be an explanation. Similar ECD experiments were performed on other doubly protonated small peptides (KRQHPG, KRDVY and TPRK). These all lead to the appearance of *c* ions as the main fragments and the peptide AGWLK thus appears to behave differently. In the ECD mechanism, neutralization of the proton induces the transfer of the hydrogen atom to the peptide backbone which is in competition with loss of a radical hydrogen. Here, the observation of a peak at *m/z* 574 in Fig. 2(c) and a fragmentation pattern similar to the one observed in CID for the singly protonated peptide can be viewed as a signature of this loss. The presence of a *w* ion, usually associated with high-energy collisions, might indicate that this neutralization/loss process leaves more energy in the system than brought by low-energy collisions. In the

DOI: 10.1002/rcm

structures of the doubly protonated pentapeptide generated with the Monte Carlo simulations, the number of NH^+-CO interactions is smaller than for the singly protonated peptide. By choosing a cut-off distance of 2.5 Å for the interaction between the proton and the carbonyl oxygen, on average only 1.1 hydrogen atoms of each NH_3^+ group are engaged in a proton-bound interaction with one of the five accessible carbonyl groups. A preferential ECD fragmentation for carbonyl groups in interaction with the protonation site was already shown on larger systems.[12] Although no Monte Carlo simulations were performed for the above-mentioned small peptides that exhibit *c* fragmentation, one could hypothesize, in line with the work by Cooper,[30] that the two charges can be localized at the same side of the peptides, allowing easier internal solvation of the charges by the carbonyl groups of the neutral side of the chain. In all these latter cases, the hydrogen transfer to a carbonyl group should be favored, leading to *c*/*z* fragmentation, whereas, in the case of the AGWLK peptide for which few carbonyl groups are in interaction with the ammonium groups, H atom loss should be favored.

CONCLUSIONS

Comparison between CID, LID and ECD on a selected pentapeptide brings surprising results. These results can be explained by the dynamics that occur just after the excitation of the peptide and which may be dependent on the secondary structure of the peptide. *Ab initio* calculations of excited states and further experiments on larger peptides and/or proteins which exhibit secondary structures are needed to validate the importance of the secondary structure on the fragmentation pathways. If this is confirmed, it opens a way to a better understanding of peptide fragmentation in particular in LID and ECD experiments and also to a possible identification of families of structures from fragmentation patterns. This work is a first step toward this goal. Our main message is that systematic CID, LID and ECD experiments on small model peptides can lead to a better understanding of the different mechanisms involved in peptide relaxation and fragmentation.

Acknowledgements

GDR CNRS 2758 'Agrégation, fragmentation et thermodynamique des systèmes complexes isolés' is acknowledged for financial support.

REFERENCES

1. Zubarev RA, Kelleher NL, McLafferty FW. *J. Am. Chem. Soc.* 1998; **120**: 3265.
2. Tabarin T, Antoine R, Broyer M, Dugourd P. *Rapid Commun. Mass Spectrom.* 2005; **19**: 2883.
3. Grégoire G, Kang H, Dedonder-Lardeux C, Jouvet C, Desfrançois C, Onidas D, Lepere V, Fayeton JA. *Phys. Chem. Chem. Phys.* 2006; **8**: 122.
4. Zubarev RA, Haselmann KF, Budnik B, Kjeldsen F, Jensen F. *Eur. J. Mass Spectrom.* 2002; **8**: 337.
5. Turecek F. *J. Am. Chem. Soc.* 2003; **125**: 5954.
6. Syrstad EA, Stephens DD, Turecek F. *J. Phys. Chem. A* 2003; **107**: 115.
7. Zubarev RA, Friddriksson EK, Horn DM, Kelleher NL, Kruger NA, Carpenter BK, McLafferty FW. *Anal. Chem.* 2000; **72**: 563.
8. Horn DM, Breuker K, Frank AJ, McLafferty FW. *J. Am. Chem. Soc.* 2001; **123**: 9792.
9. Breuker K, Oh HB, Horn DM, Cerda BA, McLafferty FW. *J. Am. Chem. Soc.* 2002; **124**: 6407.
10. Oh H, Breuker K, Sze SK, Ge Y, Carpenter BK, McLafferty FW. *Proc. Natl. Acad. Sci.* 2002; **99**: 15863.
11. Adams CM, Kjeldsen F, Zubarev RA, Budnik BA, Haselmann KF. *J. Am. Soc. Mass Spectrom.* 2004; **15**: 1087.
12. Polfer NC, Haselmann KF, Langridge-Smith PRR, Barran PE. *Mol. Phys.* 2005; **103**: 1481.
13. Kang H, Jouvet C, Dedonder-Lardeux C, Martrenchard S, Grégoire G, Desfrançois C, Schermann J-P, Barat M, Fayeton JA. *Phys. Chem. Chem. Phys.* 2005; **7**: 394.
14. Sobolewski AL, Domcke W, Dedonder-Lardeux C, Jouvet C. *Phys. Chem. Chem. Phys.* 2002; **4**: 1093.
15. Williams ER, Furlong JJP, McLafferty FW. *J. Am. Soc. Mass Spectrom.* 1990; **1**: 288.
16. Barbacci DC, Russell DH. *J. Am. Soc. Mass Spectrom.* 1999; **10**: 1038.
17. Kim T-Y, Thompson MS, Reilly JP. *Rapid Commun. Mass Spectrom.* 2005; **19**: 1657.
18. Talbot F, Tabarin T, Antoine R, Broyer M, Dugourd P. *J. Chem. Phys.* 2004; **122**: 74310.
19. Kang H, Dedonder-Lardeux C, Jouvet C, Martrenchard S, Grégoire G, Desfrançois C, Schermann JP, Barat M, Fayeton JA. *J. Chem. Phys.* 2005; **122**: 84307.
20. Arnold S, Sulkes M. *J. Phys. Chem.* 1992; **96**: 4768.
21. Dedonder-Lardeux C, Jouvet C, Perun S, Sobolewski AL. *Phys. Chem. Chem. Phys.* 2003; **5**: 5118.
22. Lakowicz JR. *Principles of Fluorescence Spectroscopy* (2nd edn). Kluwer Academic/Plenum: New York, 1999.
23. Nolting D, Marian C, Weinkauf R. *Phys. Chem. Chem. Phys.* 2004; **6**: 2633.
24. Rizzo TR, Park YD, Peteanu LA, Levy DH. *J. Chem. Phys.* 1986; **84**: 2534.
25. Yao CX, Turecek F. *Phys. Chem. Chem. Phys.* 2005; **7**: 912.
26. Swendsen RH, Wang JS. *Phys. Rev. Lett.* 1986; **57**: 2607.
27. Hansmann UHE. *Chem. Phys. Lett.* 1997; **281**: 140.
28. Cornell WD, Cieplack P, Bayly CI, Gould IR, Merz KM, Ferguson DM, Spellmeyer DC, Fox T, Caldwell JW, Kollman PA. *J. Am. Chem. Soc.* 1995; **117**: 5179.
29. Haselmann KF, Budnik BA, Kjeldsen F, Nielsen ML, Olsen JV, Zubarev RA. *Eur. J. Mass Spectrom.* 2002; **8**: 117.
30. Cooper HJ. *J. Am. Soc. Mass Spectrom.* 2005; **16**: 1932.

DOI: 10.1002/rcm